Journal of Innate Immunity

Research Article

J Innate Immun 2023;15:822–835
DOI: 10.1159/000534704

Received: April 28, 2023
Accepted: October 17, 2023
Published online: October 30, 2023

YTHDC1-Modified m6A Methylation of Hsa_circ_0102678 Promotes Keratinocyte Inflammation Induced by *Cutibacterium acnes* Biofilm through Regulating miR-146a/TRAF6 and IRAK1 Axis

Meng Zhou[a] Yuzhen Liu[b] Haoxiang Xu[a] Xu Chen[a] Nana Zheng[a] Zhimin Duan[a] Yiping Ge[a] Dongqing Li[a] Tong Lin[a] Rong Zeng[a, c] Qing Chen[d, e] Min Li[a, e]

[a]Department of Laser Surgery, Jiangsu Key Laboratory of Molecular Biology for Skin Diseases and STIs, Hospital of Dermatology, Chinese Academy of Medical Sciences and Peking Union Medical College, Nanjing, China; [b]Department of Dermatology, The Affiliated Jiangning Hospital with Nanjing Medical University, Nanjing, China; [c]Department of Dermatology, Yunnan Provincial Traditional Chinese Medicine Hospital, Kunming, China; [d]Department of Transfusion Medicine, Nanjing Drum Tower Hospital, The Affiliated Hospital of Nanjing University Medical School, Nanjing, China; [e]Center for Global Health, School of Public Health, Nanjing Medical University, Nanjing, China

Keywords
CircRNA · m6A · YTHDC1 · Acne · Inflammation · miR-146a

Abstract

Introduction: CircRNAs are closely related to many human diseases; however, their role in acne remains unclear. This study aimed to determine the role of hsa_circ_0102678 in regulating inflammation of acne. ***Methods:*** First, microarray analysis was performed to study the expression of circRNAs in acne. Subsequently, RNase R digestion assay and fluorescence in situ hybridization assay were utilized to confirm the characteristics of hsa_circ_0102678. Finally, qRT-PCR, Western blotting analysis, immunoprecipitation, luciferase reporter assay, circRNA probe pull-down assay, biotin-labeled miRNA pull-down assay, RNA immunoprecipitation assay, and m6A dot blot assay were utilized to reveal the functional roles of hsa_circ_0102678 on inflammation induced by *C. acnes* biofilm in human primary keratinocytes. ***Results:*** Our investigations showed that the expression of hsa_circ_0102678 was significantly decreased in acne tissues, and hsa_circ_0102678 was a type of circRNAs, which was mainly localized in the cytoplasm of primary human keratinocytes. Moreover, hsa_circ_0102678 remarkably affected the expression of IL-8, IL-6, and TNF-α, which induced by *C. acnes* biofilm. Importantly, mechanistic studies indicated that the YTHDC1 could bind directly to hsa_circ_0102678 and promote the export of N6-methyladenosine-modified hsa_circ_0102678 to the cytoplasm. Besides, hsa_circ_0102678 could bind to miR-146a and sponge miR-146a to promote the expression of IRAK1 and TRAF6. ***Conclusion:*** Our findings revealed a previously unknown process by which

karger@karger.com
www.karger.com/jin

© 2023 The Author(s).
Published by S. Karger AG, Basel

This article is licensed under the Creative Commons Attribution-NonCommercial 4.0 International License (CC BY-NC) (http://www.karger.com/Services/OpenAccessLicense). Usage and distribution for commercial purposes requires written permission.

Correspondence to:
Rong Zeng, zengrong2010@hotmail.com
Qing Chen, chenqing90@yahoo.com
Min Li, limin@pumcderm.cams.cn

hsa_circ_0102678 promoted keratinocyte inflammation induced by *C. acnes* biofilm via regulating miR-146a/TRAF6 and IRAK1 axis.

© 2023 The Author(s).
Published by S. Karger AG, Basel

Introduction

Acne is a common, persistent, and recurring inflammatory skin disease that affects 80–90% of adolescents and often has negative physical and psychological effects [1]. The pathophysiology of acne is complex and multifactor which includes increased production of sebum, hyperkeratinization of the sebaceous unit, *Cutibacterium acnes* (*C. acnes*) infection, and inflammation [2, 3]. However, there are few reports of the molecular mechanisms by which *C. acnes* causes acne [4]. Therefore, it is necessary to investigate the pathological mechanism of acne by establishing a model of acne via *C. acnes* in vitro.

Eukaryotic genomes, which have diverse transcriptional characteristics, can produce distinct RNA transcripts, with noncoding RNAs (ncRNAs) accounting for the majority. However, the main reports on the pathogenesis of acne were restricted to genes encoding proteins [5]. Only a few reports suggested that ncRNAs such as long noncoding RNA (lncRNA) and microRNA (miRNA) were closely associated with acne [6–8]. Apparently, there was a lack of study on the roles of ncRNAs in acne.

CircRNAs are a unique type of ncRNA molecule, which is produced by a covalent bond by back-splicing of linear RNA in eukaryotes [9]. Importantly, circRNAs could act as competitive endogenous RNAs (ceRNAs) to sponge off and regulate miRNAs on their target genes [10–12]. As reported, circRNAs played a considerable regulatory role in various diseases and were involved in the pathogenesis and progression of inflammatory skin disorders by distinct molecular mechanisms [13–15]. For example, hsa_circ_0061012 participated in psoriasis in response to NF-κB nuclear import regulations and T cell selection, which may be a potential biomarker for psoriasis [14]. Additionally, transcriptional profiling of circRNAs in severe acne and adjacent to the patient's normal skin tissues showed that 538 differently expressed of circRNAs were associated with the occurrence and development of acne [16]. However, the underlying biological functions and molecular mechanisms of circRNAs in acne remain unexplained.

The RNA modification of N6-methyladenosine (m6A) was widely present in eukaryotes, which was included demethylases (the "eraser"), methyltransferases (the "writer"), and m6A-binding proteins (the "reader") [17, 18]. YTH domain-containing 1 (YTHDC1), an m6A-reader protein, has been linked to physiological and pathophysiology processes in several diseases by regulating the nuclear export of mRNA [19, 20]. Nevertheless, recent reports mainly focused on how m6A modification regulated tumorigenesis [21–23], and studies of m6A modification in the pathogenesis and progression of acne were missing.

In this study, we attempted to investigate whether hsa_circ_0102678 could sponge miR-146a to induce activation of the innate immune response, and positively regulated of IRAK1 and TRAF6 in human primary keratinocytes in vitro acne model. Moreover, we hypothesized that hsa_circ_0102678 was exported to the cytoplasm by binding to YTHDC1 in a methylated m6A-dependent manner. In summary, our research tried to reveal the function and mechanism of hsa_circ_0102678 in acne.

Materials and Methods

Microarray Analysis

Clinical tissue samples were obtained from 12 volunteers (online suppl. Table 1; for all online suppl. material, see https://doi.org/10.1159/000534704). The samples have been pretreated and hybridized with Aksomics (Shanghai, China). After digesting circular RNAs with RNase R (Epicenter Technologies, Madison, WI, USA) to remove linear RNAs, amplified circular RNAs were then transcribed into fluorescent circRNA using the Arraystar Super RNA Labeling Kit (Arraystar). The tagged circRNAs were hybridized onto the Arraystar Human circRNA Array V2 (8 15 K, Arraystar), followed by scanning with the Agilent Scanner G2505C (Jamul, CA, USA). Agilent scanner G2505C was used to detect the hybrid array. Microarray data were downloaded from Gene Expression Omnibus (GSE212605).

Cell Cultures and Stimulation

Human primary keratinocytes were obtained from foreskin tissue of young persons under 12 years of age, and the detailed experimental procedure was described in [24]. The *C. acnes* biofilm was inactivated at 80°C for 30 min. When the cell density was above than 90%, *C. acnes* biofilm was added and incubated for 6 or 24 h. Our previously study had performed specific processes [7].

RNA Extraction, RNase R Treatment, and Quantitative Reverse Transcriptase-Polymerase Chain Reaction

Total RNA was extracted using TRIzol reagent (Invitrogen, USA). Besides, 2 μg total RNA was treated with ^{3} U/μ^{g} of RNase R (Geneseed, China) at 37°C for 15 min, followed by synthesizing cDNA with First Strand cDNA Synthesis Kit (Thermo Scientific, USA) and RT-PCR examination using SYBR Green SuperMix (YEASEN, China). U6 or GAPDH was used as control. The primers were listed in online supplementary Table 2.

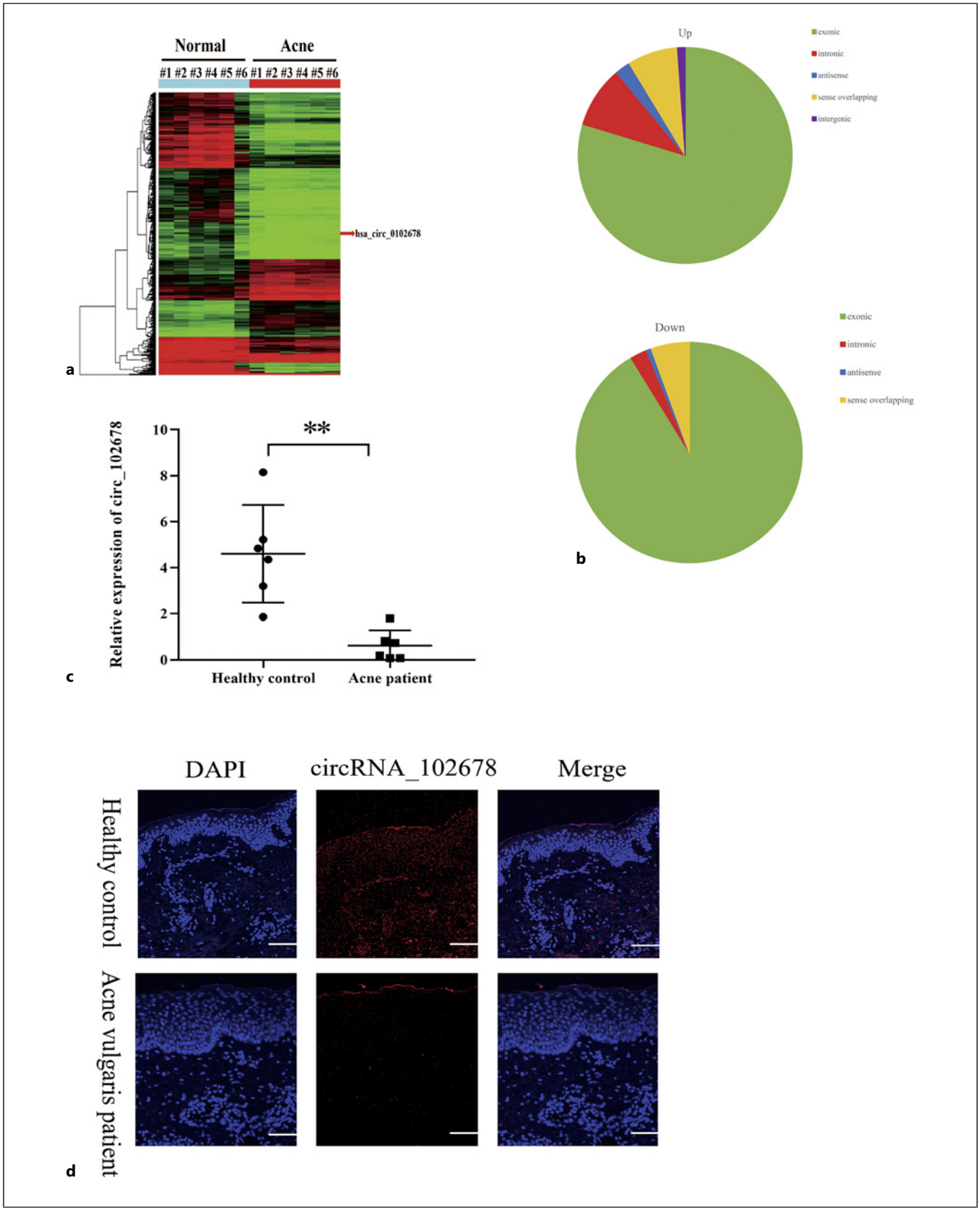

1

(For legend see next page.)

J Innate Immun 2023;15:822–835
DOI: 10.1159/000534704

Plasmids, Short Interfering RNAs, and Cell Transfection

The circRNA overexpression plasmid (pcDNA3.1 CircRNA Mini) was purchased from MiaolingBio (Wuhan, China). Hsa_circ_0102678 or control short interfering RNA (siRNA) (50 nM, General Biosystems, China) was transfected into human primary keratinocyte. The hsa_circ_0102678 sequence was cloned into pcDNA3.1 circRNA vector (Miaoling, China) by EcoRI and NotI cleavage sites, and then hsa_circ_0102678 overexpression plasmid was obtained. All siRNAs and plasmids were transfected into keratinocytes using jetPRIME (Polyplus, France), as instructed by the manufacturer. The siRNA sequences are shown in online supplementary Table 3.

Western Blotting Assay

Cell lysates were collected by RIPA lysis buffer (Beyotime, China) with 1× protease inhibitors and phosphorylase inhibitors (Thermo Fisher, USA). Western blotting (WB) was performed as previously described [25]. Immunoreactive results were envisaged using a stationary enhanced chemiluminescence kit (YEASEN, Shanghai, China) on a Bio-Rad gel imaging system. The antibodies used were listed in online supplementary Table 4.

RNA Fluorescence in situ Hybridization Assay

5′-FAM-labeled hsa_circ_0102678 and control probe sequence were designed and synthesized from Gene Pharma (Shanghai, China). The fluorescence in situ hybridization (FISH) kit (Gene Pharma, Shanghai, China) was used for hybridization analysis. Briefly, tissues or human primary keratinocytes were fixed in 4% paraformaldehyde. The slices were hybridized with specific probes at 37°C in a dark damp room. The slices were then sealed with paraffin containing DAPI. Confocal laser scanning microscope (Olympus FV1000) was performed to capture the images.

Immunofluorescence Assay

Human primary keratinocytes grew on the confocal dish (Corning, USA) and were fixed with 4% paraformaldehyde for 20 min. Subsequently, the cells were permeabilized in 0.1% TritonX-100 and washed thrice with PBS. After blocking with 5% normal goat serum for 1 h at 37°C, the cells incubated with primary antibody overnight at 4°C and then incubated with secondary antibodies for 1 h at 37°C. DAPI was utilized to stain nuclear. Fluorescent micrograph images were captured by a confocal laser scanning microscope (Olympus FV1000). The antibodies used were listed in online supplementary Table 4.

Luciferase Reporter Assay

The pGL3 Basic luciferase reporter vector was purchased from Tsingke (Nanjing, China). The wild-type and mutant sequences of hsa_circ_0102678 encoding the expected miR-146a binding site were cloned into pGL3 vector. These recombinant luciferase reporter plasmids were co-transfected into human primary keratinocytes with miR-146a mimics, inhibitors, or controls. Luciferase activity levels inside transfected cells were determined by a dual-luciferase assay system (Promega, E2920, USA).

RNA Immunoprecipitation Assay

The EZ Magna RNA immunoprecipitation Kit (Millipore, USA) was used for RNA immunoprecipitation (RIP) analysis. Briefly, human primary keratinocytes were lysed in RIP lysis buffer after miR-146a mimics transfection for 48 h. Magnetic beads were pre-incubated with Ago2 antibody overnight at 4°C. IgG was used as a negative control. The cell lysates were immunoprecipitated with beads at 4°C for 6 h. The coprecipitated RNAs were then purified and detected by quantitative reverse transcriptase-polymerase chain reaction (qRT-PCR). The input fraction Ct value was used to normalize the RNA sample preparation differences in each group, and the negative controls (IgG) Ct were used to adjust background fraction.

CircRNA Probe Pull-Down Assay

First, the 3′-end biotinylated hsa_circ_0102678 or control probe was incubated with C-1 magnetic beads (Life Technologies, USA) for 3 h at room temperature. Then, C-1 magnetic beads were incubated with cell lysates at 4°C for 12 h. Finally, the results were analyzed by WB assay and qRT-PCR assay. Biotinylated hsa_circ_0102678 probes and control probes were listed in online supplementary Table 5.

Biotin-Labeled miRNA Pull-Down Assay

The 3′-end biotinylated miR-146a mimics or the miRNA control (50 nM, General Biosystems, Anhui, China) was transfected into human primary keratinocytes for 48 h. Next, the cell lysates were harvested. Then Dynabeads MyOne Streptavidin C1 kit (Invitrogen, USA) was applied to enrich the biotin-coupled RNA combination. To remove unbound materials, the beads were pelleted and washed. The TRIzol reagent was used to extract RNA that was bound to beads. qRT-PCR was used to test the abundance of hsa_circ_0102678 in the isolated fractions. All sequences were listed in online supplementary Table 5.

m6A Dot Blot Assay

RNA was extracted from human primary keratinocytes using TRIzol and then degenerated at 95°C for 3 min. Nitrocellulose membrane (Amersham, GE Healthcare, USA) was used to spot RNAs, following by under ultraviolet light for 30 min. After dyeing with 0.02% methylene blue (Sangon Biotech, China), the membranes were blocked with 5% bovine serum albumin for 1 h at 25°C and incubated with m6A antibody (Proteintech, China) overnight at 4°C. The next day, the membranes were with secondary antibodies for 1 h at room temperature. The results were tested by ECL chemiluminescence (Bio-Rad, USA).

Fig. 1. Hsa_circ_0102678 was downregulated in acne patients. **a** Hierarchically clustered heat map was used to visualize differential circRNAs between acne and control skin tissues from the control cohort (n = 6) and acne patients (n = 6). The red color indicated upregulated circRNAs and green color indicated downregulated circRNAs. **b** Classification of differential circRNAs. **c** qRT-PCR analysis of hsa_circ_0102678 expression in acne and matched adjacent normal tissue patients. **d** RNA-FISH analysis of hsa_circ_0102678 expression in acne and matched adjacent normal tissue patients. Hsa_circ_0102678 (red); DAPI stained to the nucleus (blue). Scale bars: 10 μm. Student's t test: $^{**}p < 0.01$.

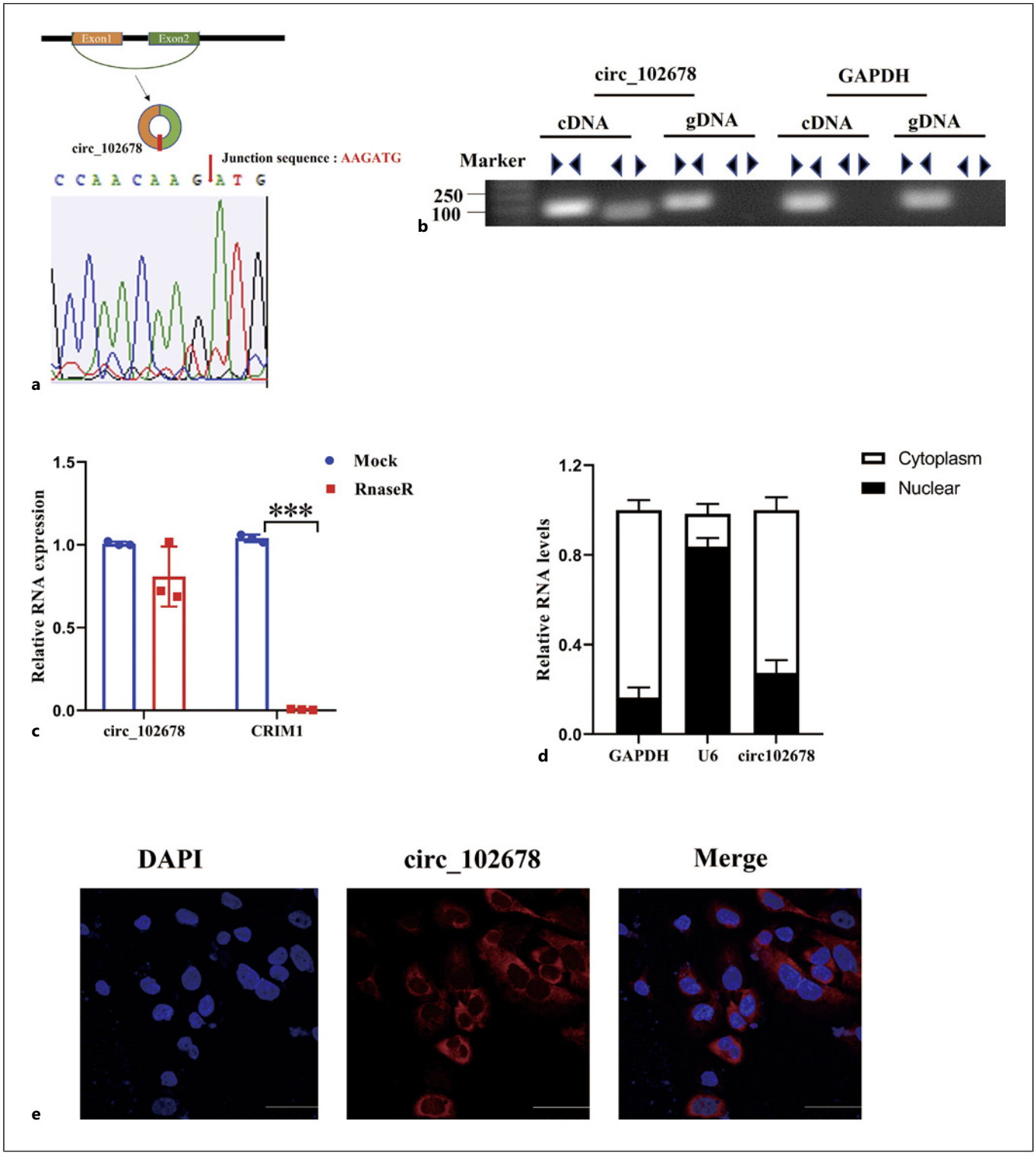

Fig. 2. Characteristics of hsa_circ_0102678 in human primary keratinocytes. **a** Schematic diagram of hsa_circ_0102678 genome locus in CRIM1 exon region. **b** Relative levels of hsa_circ_0102678 in cDNA and genomic DNA (gDNA). GAPDH was used as negative control. **c** mRNA levels of *CRIM1* and hsa_circ_0102678 with or without RNase R. **d** qRT-PCR analysis of the subcellular distribution of hsa_circ_0102678 in human primary keratinocytes. **e** FISH analysis of the subcellular distribution of hsa_circ_0102678 in human primary keratinocytes. Scale bars: 50 μm. Student's *t*-test: $^{***}p < 0.001$.

J Innate Immun 2023;15:822–835
DOI: 10.1159/000534704

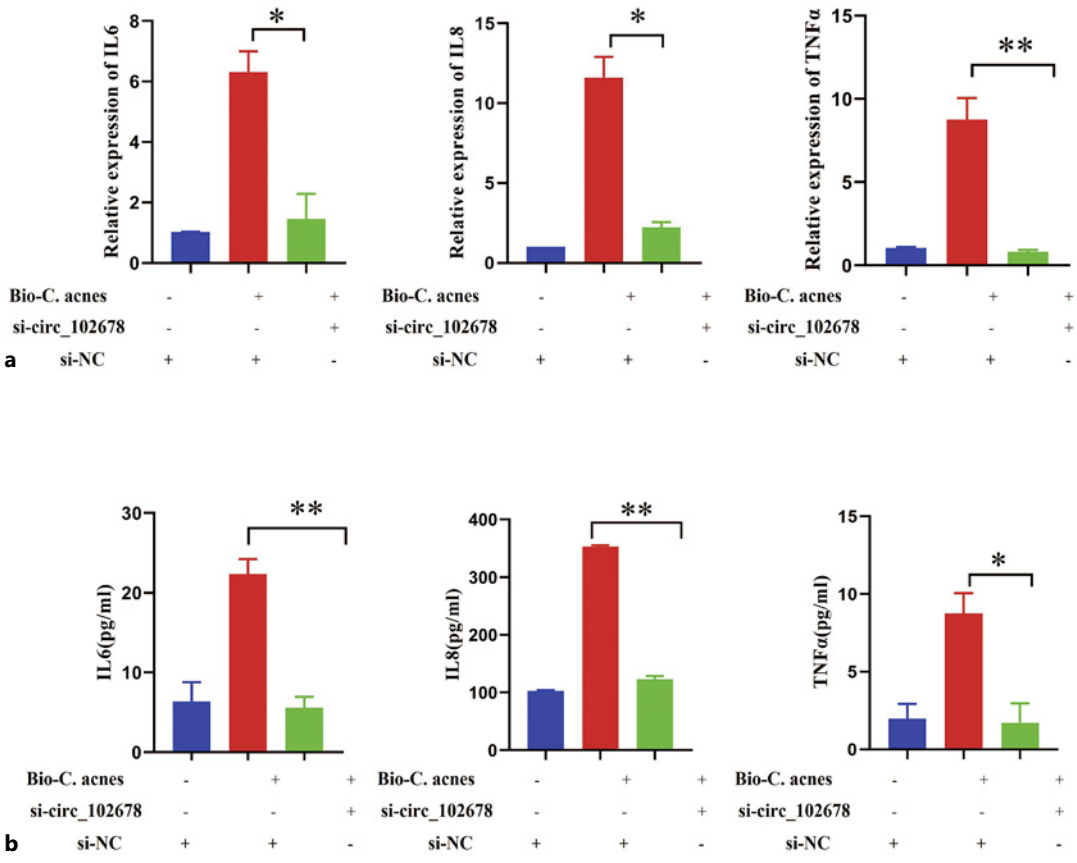

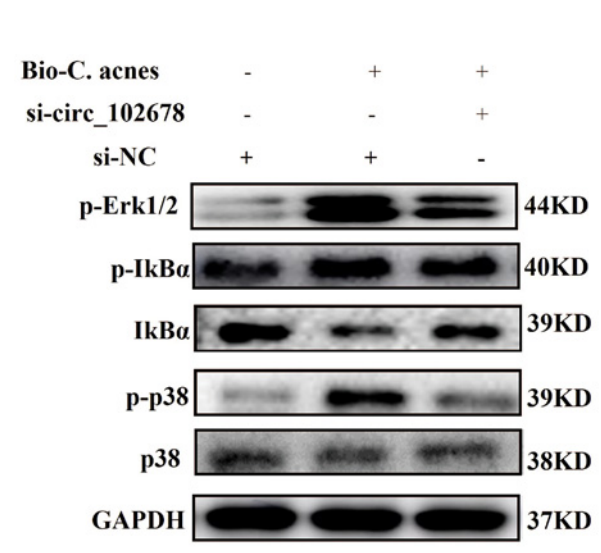

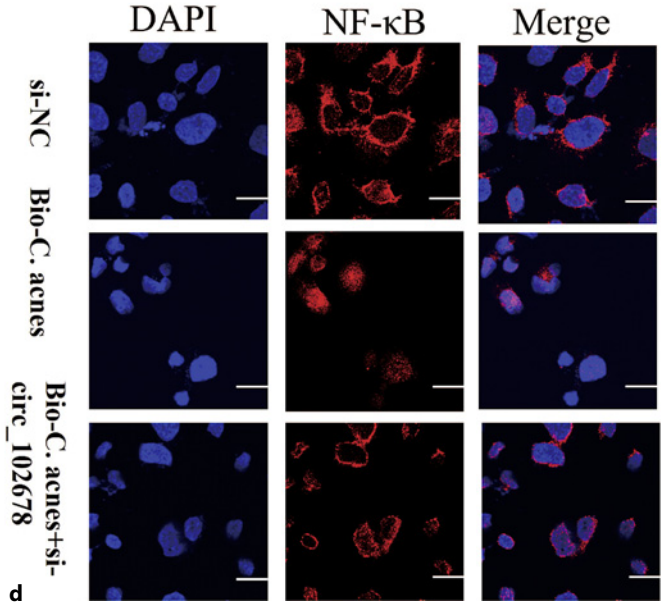

3

(For legend see next page.)

Statistical Analysis

All data were derived from three separate experiments. Statistical analyses were presented as mean ± standard deviation. Student's two-tailed t test was used to calculate statistical significance. The statistical significance limit was set at $p < 0.05$. All calculations were done using GraphPad Prism (version 6.0) software.

Results

Hsa_circ_0102678 Was Downregulated in Acne Patients

To assess the abnormal expression of circRNAs in acne, we first showed by microarray test analyses that 605 circRNAs were highly elevated, and 989 were significantly downregulated in acne tissues ($n = 6$) compared with normal tissues ($n = 6$) (fold change≥ 2 and $p < 0.05$) (Fig. 1a). Alternatively, most of the circRNAs included in these test data were composed of exons (Fig. 1b). Our previous study demonstrated that miR-146a was overexpressed and regulated inflammatory response in acne lesions [7]. To clarify whether circRNAs regulated the expression of miR-146a, we performed Cytoscape software (version 3.4.0) to evaluate the potential circRNAs. Hsa_circ_0102678 attracted our attention as it was the most downregulated circRNA among three predicted circRNAs (hsa_circ_0102678, hsa_circ_0102680, hsa_circ_0105040). Indeed, we showed by qRT-PCR analyses that hsa_circ_0102678 expression levels were lower in acne tissues compared to that in adjacent normal samples (Fig. 1c). Subsequent histological analysis confirmed a clear decrease in acne tissues compared with the matched adjacent normal tissues (Fig. 1d). These findings revealed that hsa_circ_0102678 might have a potential function in pathological of acne and should be explored further.

Characteristics of hsa_circ_0102678 in Human Primary Keratinocytes

Hsa_circ_0102678 was derived from head-to-tail splicing of exon 1/2 (538 bp) of cysteine-rich transmembrane BMP regulator 1 (*CRIM1*) (Fig. 2a). To characterize the molecular features of hsa_circ_0102678, we first performed divergent and convergent primers to produce the *CRIM1* mRNA and hsa_circ_0102678 by qRT-PCR. Electrophoresis on an Agarose gel analysis confirmed that hsa_circ_0102678 was only found in cDNA and not in gDNA (Fig. 2b). Subsequently, the RNase R degradation assay confirmed that hsa_circ_0102678 did not degrade, whereas the *CRIM1* mRNA level decreased sharply (Fig. 2c). Furthermore, nuclear and cytoplasmic fractionation and FISH assay suggested that hsa_circ_0102678 was predominantly in the cytoplasm (Fig. 2d, e). Overall, our data indicated that hsa_circ_0102678 was a stable circRNA expressed in the cytoplasm of keratinocytes.

Hsa_circ_0102678 Promoted Inflammatory Response Induced by C. acnes Biofilm in Human Primary Keratinocytes

It was well acknowledged that the inflammatory response induced by *C. acnes* was related to the process of acne [26, 27]. To explore whether hsa_circ_0102678 was involved in acne via regulating inflammatory response, we first constructed a feasible model of *C. acnes* biofilm in vitro. The optical density of *C. acnes* biofilm formation was the highest on the 8th day, suggesting that 8 days might be the most suitable stimulation time for the establishment acne model (online suppl. Fig. 1a, b). Subsequently, hsa_circ_0102678 siRNA (si-circ_0102678) and the control siRNA (siNC) or overexpression hsa_circ_0102678 plasmid (pcDNA-circ_102678) and the empty control plasmid (pcDNA-circ-NC) (online suppl. Fig. 2a, b) were effectively transfected into keratinocytes, respectively. The qRT-PCR and enzyme-linked immunosorbent assay analysis prompted that knockdown of hsa_circ_0102678 significantly reduced the expression of TNF-α, IL-6, and IL-8 (Fig. 3a, b), while overexpression of hsa_circ_0102678 increased these inflammatory gene expression (online suppl. Fig. 3a, b). Meanwhile, si-circ_0102678 transfection obviously alleviated the positive impact of *C. acnes* biofilm on p-P38, p-IκBα, and p-ERK1/2 expression (Fig. 3c). Consistently, the expression of these inflammatory genes was dramatically upregulated with pcDNA-circ_102678 transfection (online suppl.

Fig. 3. Silencing hsa_circ_0102678 inhibited inflammatory response induced by *C. acnes* biofilm in human primary keratinocytes. Relative mRNA levels (**a**) and protein levels (**b**) of IL-6, IL-8, and TNF-α in human primary keratinocytes transfected with hsa_circ_0102678 or control siRNA upon ×2 × 10^8 CFU/mL heat-inactivated *C. acnes* biofilm. **c** Relative p-IκBα, IκBα, p-P38, P38, and p-ERK1/2 protein expression in human primary keratinocytes transfected with hsa_circ_0102678 or control siRNA upon ×2 × 10^8 CFU/mL heat-inactivated *C. acnes* biofilm. **d** Representative images of NF-κB P65 in human primary keratinocytes transfected with hsa_circ_0102678 or control siRNA upon ×2 × 10^8 CFU/mL heat-inactivated *C. acnes* biofilm. Scale bars: 5 μm. Bio-*C. acnes*, *C. acnes* biofilm; si-NC, scrambled control; si-circ_102678, hsa_circ_0102678 siRNA. Student's t test: $^*p < 0.05$, $^{**}p < 0.01$.

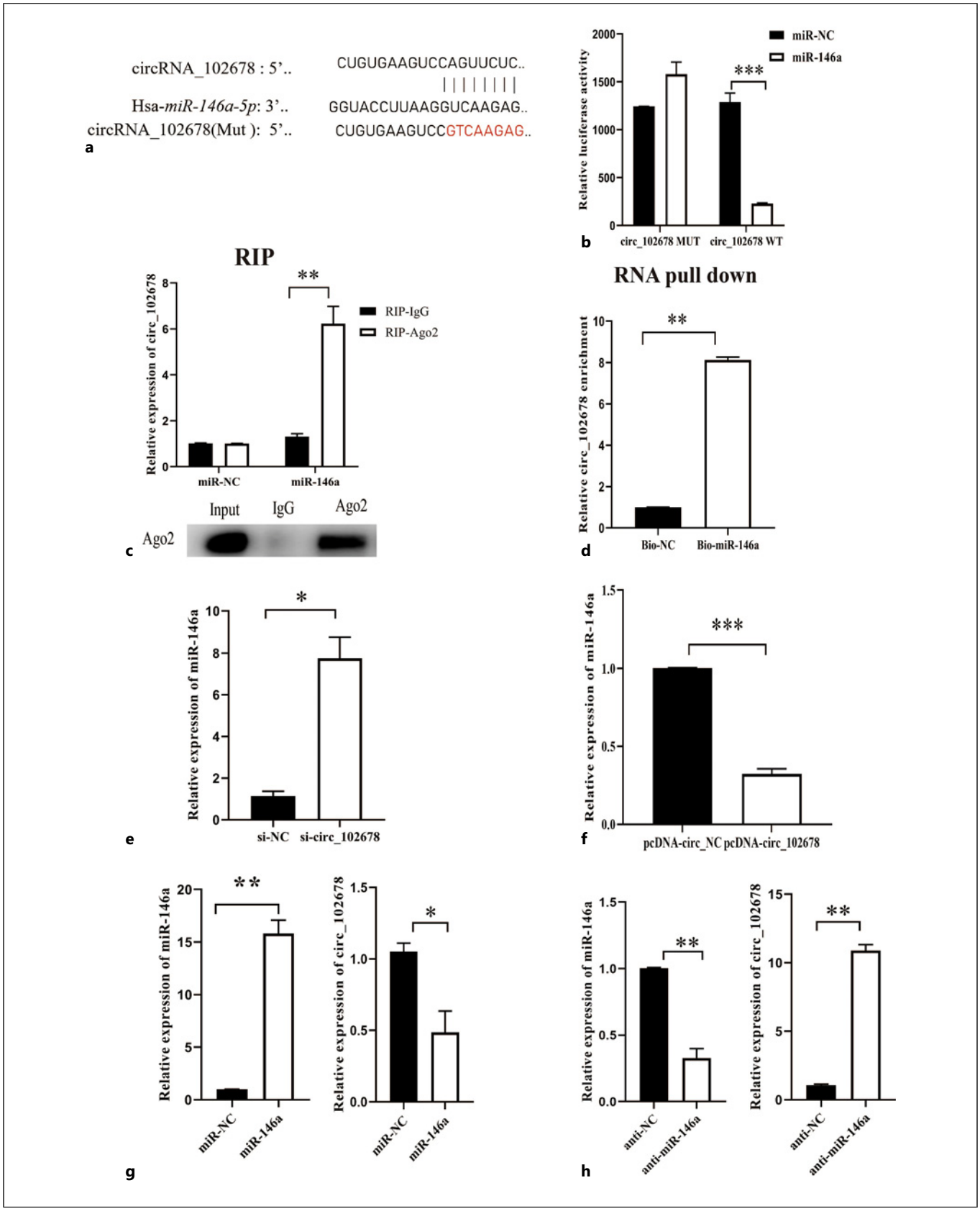

4

(For legend see next page.)

Fig. 3c). Moreover, immunofluorescence analysis showed that hsa_circ_0102678 affected *C. acnes* biofilm-induced NF-κB-p65 nuclear translocation (Fig. 3d; online suppl. Fig. 3d). In brief, these findings indicated that hsa_circ_0102678 facilitated inflammatory response in human primary keratinocytes through MAPK and NF-κB pathways.

Hsa_circ_0102678 Acted as a ceRNA to Competitively Sponge miR-146a in Human Primary Keratinocytes

As reported, cytoplasmic circRNAs functioned as ceRNAs to sponge microRNAs that specifically inhibited the expression of target mRNAs [28, 29]. Therefore, we investigated whether hsa_circ_0102678 exhibited similar effects in keratinocytes. Our previous study reported that miR-146a downregulated the expression of IL-6, IL-8, and TNF-α in acne [7]. Consequently, we attempted to further clarify the interaction between hsa_circ_0102678 and miR-146a. Indeed, bioinformatics instruments predicted that hsa_circ_0102678 might bind to miR-146a (Fig. 4a). Furthermore, luciferase experiment demonstrated that hsa_circ_0102678 could bind directly to miR-146a (Fig. 4b). Meanwhile, RIP assay evidenced that hsa_circ_0102678 existed in Ago2-containing miRNA ribonucleoprotein complexes via interacting with miR-146a (Fig. 4c). More than that, biotin-labeled miRNA pull-down assays demonstrated a significant increase of hsa_circ_0102678 expression transfected with biotin-labeled miR-146a compared to Bio-NC control (Fig. 4d). Furtherly, knockdown of hsa_circ_0102678 markedly increased the expression of miR-146a, while overexpression of hsa_circ_0102678 decreased the expression of miR-146a (Fig. 4e, f). Additionally, hsa_circ_0102678 expression was decreased with miR-146a transfection but elevated with anti-miR-146a transfection (Fig. 4g, h), manifesting that hsa_circ_0102678 might be directly bound to miR-146a. Together, these findings suggested that hsa_circ_0102678 functioned as a ceRNA for miR-146a in human primary keratinocyte cells.

Hsa_circ_0102678 Sponged miR-146a to Alleviate Targeted IRAK1 and TRAF6

As reported, *IRAK1* and *TRAF6* exerted function as the downstream target for miR-146a in the inflammatory response induced by *C. acnes* biofilm [7]. Similarly, our data showed that knockdown of hsa_circ_0102678 restricted the expression of IRAK1 and TRAF6 (Fig. 5a, b). Consistently, anti-miR-146a transfection increased IRAK1 and TRAF6, while silencing hsa_circ_0102678 could effectively alleviate positive effects of anti-miR-146a on IRAK1 and TRAF6 (Fig. 5c). Besides, the expression of TNF-α, IL-8, and IL-6 induced by *C. acnes* biofilm was increased with anti-miR-146a but decreased with si-circ_102678 (Fig. 5d, e). Taken together, these results confirmed that hsa_circ_0102678 decoyed miR-146a to upregulate *IRAK1* and *TRAF6* and promoted inflammation induced by *C. acnes* biofilm in human primary keratinocytes.

YTHDC1 Enhanced Cytoplasmic Transport of m6A Methylated hsa_circ_0102678

It was reported that m6A modification was involved in maintaining the stability and expression of eukaryotic mRNAs and noncoding RNAs [30]. Here, we first identified two highly reliable m6A sites in hsa_circ_0102678 by online bioinformatic tools (http://www.cuilab.cn/sramp/) (online suppl. Fig. 4a). Then, we identified 12 RNA-binding potential proteins that could bind to hsa_circ_0102678 via online bioinformatic tools (http://rbpdb.ccbr.utoronto.ca/). Among them, YTHDC1 protein attracted our specific attention since it was the only m6A-related RNA-binding protein [31]. These results demonstrated that hsa_circ_0102678 might have m6A modifications.

Furtherly, qRT-PCR analysis showed that *YTHDC1* was dramatically decreased in acne compared to adjacent normal tissues (online suppl. Fig. 4b). Correspondingly, the expression of YTHDC1 was suppressed with *C. acnes* biofilm in a temporal manner in human primary keratinocytes (Fig. 6a). Surprisingly, hsa_circ_0102678 was substantially enriched with YTHDC1 than the control probe

Fig. 4. Hsa_circ_0102678 acted as a ceRNA and competitively sponged miR-146a in human primary keratinocytes. **a** Prediction of miR-146a binding sequence at hsa_circ_0102678. The mutated sequence showed red nucleotides. **b** Luciferase assay analysis of hsa_circ_0102678 or mutant luciferase activity in human primary keratinocytes transfected with miR-146a or control mimics. **c** RIP analysis of hsa_circ_0102678 relative fold enrichment in human primary keratinocytes. Ago2 protein was used to detect RIP reliability by WB analysis. IgG was used as a negative control. **d** Enrichment of hsa_circ_0102678 in human primary keratinocytes transfected with biotin-miR-146a or miR-NC by miR-146a pull-down assay. **e** qRT-PCR analysis of miR-146a expression in human primary keratinocytes transfected with hsa_circ_0102678 or control siRNA. **f** qRT-PCR analysis of miR-146a expression in human primary keratinocytes transfected with hsa_circ_0102678 plasmid or empty control plasmid. **g** qRT-PCR analysis of miR-146a (left) and hsa_circ_0102678 (right) in human primary keratinocytes transfected with miR-146a or miR-NC mimics. **h** qRT-PCR analysis of miR-146a (left) and hsa_circ_0102678 (right) in human primary keratinocytes transfected with anti-miR-NC or anti-miR-146a. Student's *t* test: $^{*}p < 0.05$, $^{**}p < 0.01$, $^{***}p < 0.001$.

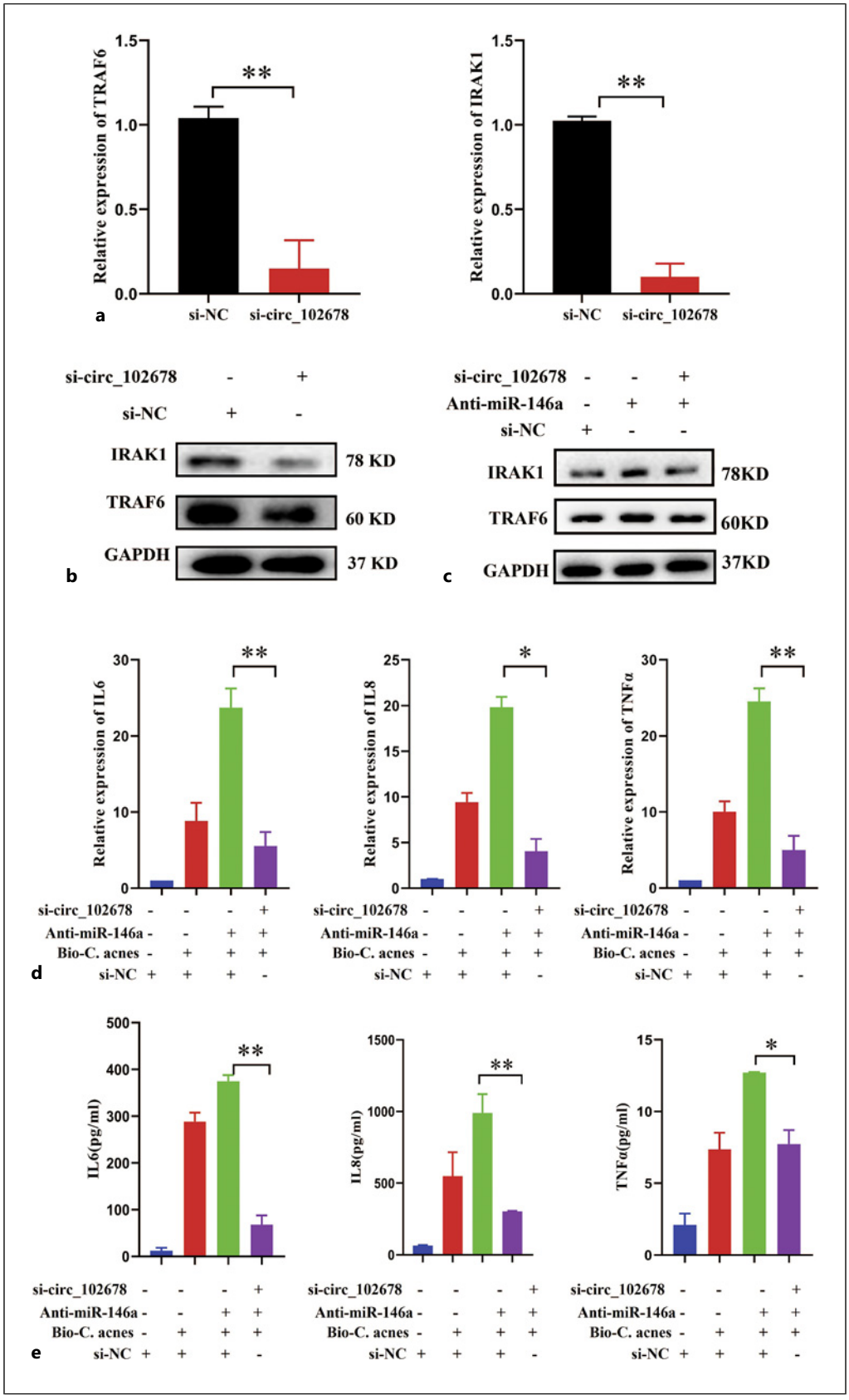

Fig. 5. Hsa_circ_0102678 sponged miR-146a to alleviate targeted IRAK1 and TRAF6. Relative TRAF6 and IRAK1 mRNA (**a**) and protein expression (**b**) in human primary keratinocytes transfected with hsa_circ_0102678 or control siRNA. **c** WB analysis of TRAF6 and IRAK1 expression in human primary keratinocytes under the specified circumstances. Relative IL-6, IL-8, and TNF-α mRNA (**d**) and protein expression (**e**) in human primary keratinocytes under the specified circumstances. Student's *t* test: $*p < 0.05$, $**p < 0.01$.

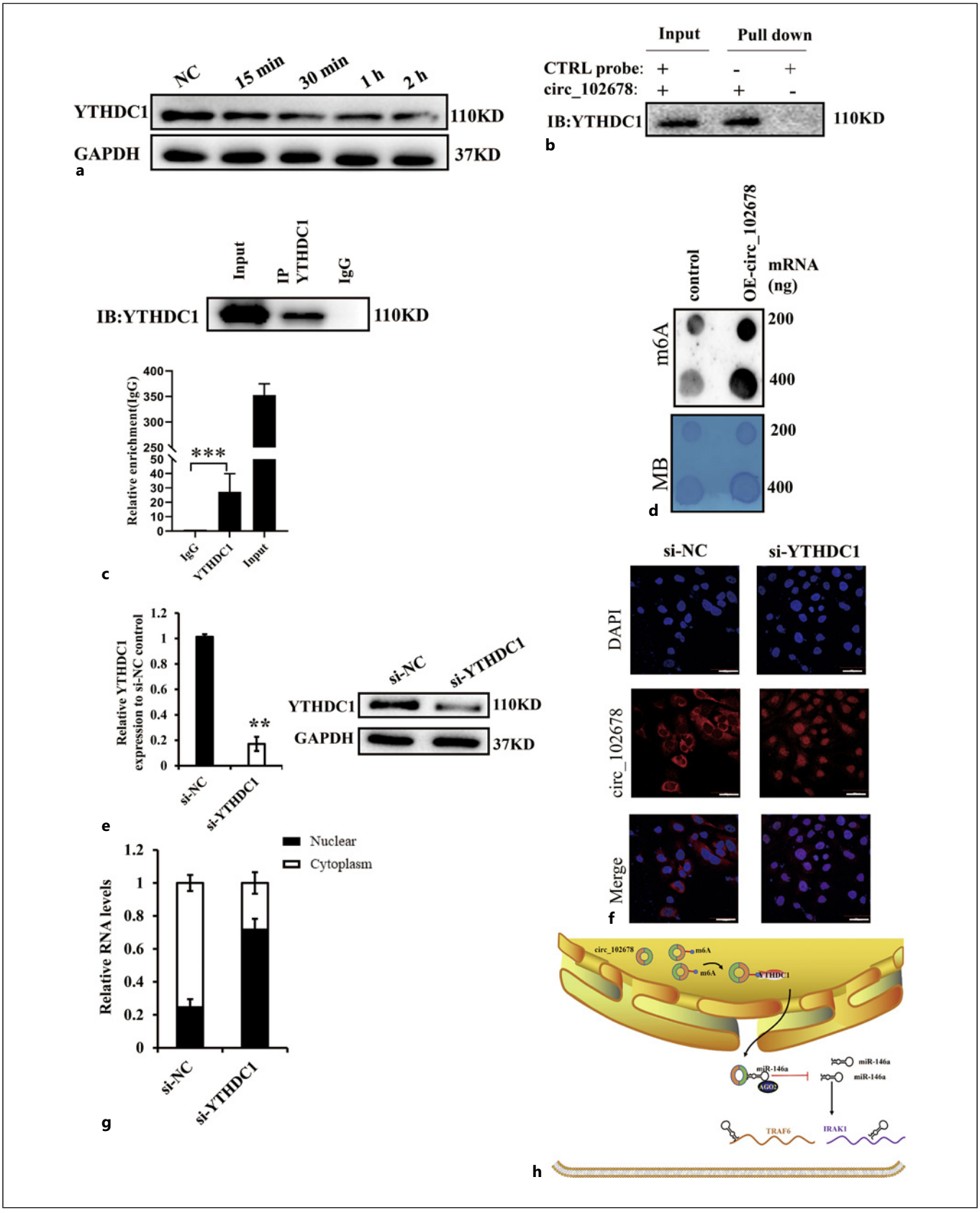

6

(For legend see next page.)

immunoprecipitants, indicating that hsa_circ_0102678 may have a relationship with YTHDC1 (Fig. 6b). In addition, complex precipitation of YTHDC1 antibodies significantly enriched hsa_circ_0102678 compared with immunoprecipitant control IgG (Fig. 6c). These findings suggested that YTHDC1 had potential for interaction with hsa_circ_0102678.

To probe whether YTHDC1 regulated hsa_circ_0102678 through m6A modification, we first performed dot blot assays to assess m6A levels. As shown in Figure 6d, overexpression of hsa_circ_0102678 increased the level of m6A in human primary keratinocytes. As reported, YTHDC1 could promote the nuclear export of m6A-modified circRNAs [32]. Here, we utilized siRNAs to interfere with YTHDC1 expression in human primary keratinocytes at the mRNA and protein expression levels (Fig. 6e). Subsequently, FISH and nuclear and cytoplasmic fractionation analysis confirmed that knockdown of YTHDC1 dramatically increased the level of hsa_circ_0102678 in the nucleus (Fig. 6f, g). Together, these results indicated that YTHDC1 could directly bind to hsa_circ_0102678 and promote the export of hsa_circ_0102678 from the nucleus to the cytoplasm by m6A modification.

Discussion

It was well acknowledged that cellular inflammation was responsible for the occurrence and development of acne [26, 33, 34]. Meanwhile, circRNAs have appeared as a critical moderator regulating cell inflammation in many human diseases [15, 16, 35, 36]. However, there was a lack of circRNA research in the pathological process of acne. Here, we have surprisingly identified abundant circRNAs in acne and normal skin tissues. Moreover, we found that hsa_circ_0102678 promoted inflammatory reaction upon *C. acnes* biofilm in human primary keratinocytes. Mechanically, we first demonstrated that, in the process of acne pathology, YTHDC1 mediated the hsa_circ_0102678 nucleus to the cytoplasm by m6A modification. Hsa_circ_0102678 inhibited miR-146 expression and alleviated the miR-146a negative effect of TRAF6 and IRAK1, which enhanced cellular inflammation through *C. acnes* (Fig. 6h). These findings showed that hsa_circ_0102678 was an essential inflammatory gene that regulated the progression of acne.

CircRNAs were single-stranded covalent RNA molecules, which involved in occurrence, progression, and prognosis of different diseases [37–40]. Besides, it was supposed that dysregulation of circRNAs might contribute to inflammatory skin diseases [14, 15, 41]. Clinically, *C. acnes* infection caused skin inflammation [42–44], while whether circRNAs exerted biological functions in the process was unclear. The only accessible hint was RNA sequencing analysis of circRNA expression profile in severe acne, indicating that circRNAs might be related to immune responses and inflammation [16]. Here, we confirmed by circRNA microarray that hsa_circ_0102678 regulated inflammation in acne, which could support this study and facilitate a deeper understanding of the novel functional connections between circRNAs and acne pathogenesis.

As reported, circRNAs could exert as ceRNA to bind miRNAs, leading to an inhibition of their activity [10]. Additionally, more and more studies have shown that the circRNA-miRNA-mRNA interaction network plays an important role in a variety of diseases [45]. For example, Qiao et al. [46] revealed that circRNA_0048211 could bind to miRNA-93-5p and was negatively correlated with miRNA-93-5p and positively correlated with BMP2 (BMP2 was a direct target of miRNA-93-5p), thus alleviating the progression of postmenopausal osteoporosis. Moreover, similar findings have been reported in breast cancer [47], diabetic nephropathy [48], osteoarthritis [49], cutaneous squamous cell carcinoma [50], and arthritis [51]. In parallel with these reports, our studies showed that hsa_circ_0102678 expression was inversely correlated with miR-146a expression in acne, but this correlation was positive with IRAK1 and TRAF6, indicating that hsa_circ_0102678 might sponge miR-146a to regulate inflammation in acne.

Fig. 6. YTHDC1 enhanced cytoplasmic transport of m6A methylated hsa_circ_0102678. **a** WB analysis of YTHDC1 in human primary keratinocytes upon heat-inactivated *C. acnes* biofilm at the indicated time points. **b** Enrichment of YTHDC1 in human primary keratinocytes by miR-146a pull-down assay. **c** RIP analysis of YTHDC1 relative fold enrichment in human primary keratinocytes. Top, YTHDC1 protein was used to detect RIP reliability by WB analysis. IgG was used as a negative control. Bottom, relative expression of hsa_circ_0102678 was analyzed by qRT-PCR. **d** m6A dot blot assay analysis of m6A expression in human primary keratinocytes transfected with hsa_circ_102678 overexpression or control plasmid. **e** Relative *YTHDC1* mRNA (left) and YTHDC1 protein (right) levels in human primary keratinocytes transfected with YTHDC1 or control siRNA. **f** RNA-FISH assay analysis of hsa_circ_0102678 in human primary keratinocytes transfected with YTHDC1 or control siRNA. Scale bars: 50 μm. **g** qRT-PCR analysis of the subcellular distribution of hsa_circ_0102678 in human primary keratinocytes transfected with YTHDC1 or control siRNA. **h** A proposed model for hsa_circ_0102678/miR-146a/TRAF6/IRAK1 axis in regulating inflammatory response in human primary keratinocytes. Student's *t* test: $^{**}p < 0.01$, $^{***}p < 0.001$.

Previous studies had shown that m6A modification was related to transcription, processing, splicing, degradation, and translation of RNA. Recently, a study had investigated that YTHDC1 could bind to circNSUN2 and facilitate the transport of circNSUN2 from the nucleus to the cytoplasm in an m6A-dependent manner [21]. Coincident with this report, our study also confirmed that YTHDC1 could interact with hsa_circ_0102678, which promoted the transport of hsa_circ_0102678 from the nucleus to the cytoplasm in human primary keratinocytes. Additionally, we evidenced that the line expression profile of YTHDC1 as that of hsa_circ_0102678 in acne compared to normal skin tissue, furtherly suggesting that YTHDC1 possibly functioned as a significant upstream regulator on hsa_circ_0102678/miR-146a/TRAF6/IRAK1 axis.

In our study, we confirmed the significant low expression of hsa_circ_0102678 in acne tissues, which provided a biomarker for auxiliary diagnosis of acne and offered a potential target for the development of new drugs for acne. We have reported for the first time that hsa_circ_0102678 was involved in acne disease, providing a reference for a better understanding of the pathological mechanism of acne. In the future, we will attempt to explore whether hsa_circ_0102678 is involved in other inflammatory skin diseases similar to acne. Of course, our research also has some limitations. In this study, we recruited 12 volunteers, including 6 healthy volunteers and 6 acne patients. Therefore, the number of clinical samples we collected was not large enough, and there was a lack of samples from female. In the future, we will collect enough clinical samples from both male and female to continue scientific research in acne diseases.

Collectively, our work uncovered a novel mechanism by which hsa_circ_0102678 exported to the cytoplasm through YTHDC1 and exerted the inhibition of miR-146a on TRAF6 and IRAK1, resulting in elevated levels of inflammation. Our study might provide new insights into the mysteries of occurrence and pathogenesis in acne, which highlighted the underlying clinical value of hsa_circ_0102678/miR-146a/TRAF6/IRAK1 axis in the diagnosis and treatment of acne.

Acknowledgments

We were very grateful to donors for their participation and cooperation in providing us with important clinical evidence.

Statement of Ethics

This investigation followed the Declaration of Helsinki's criteria. The Medical Ethics Committee of the Hospital of Dermatology, Chinese Academy of Medical Sciences, approved this study, and all participants or participants' parents gave written informed consent for participation in our clinical study (Grant No. 2018-KY-012).

Conflict of Interest Statement

The authors have no conflicts of interest to declare.

Funding Sources

This study was supported by National Natural Science Foundation of China (81773338, 82103749, 82272294); CAMS Innovation Fund for Medical Sciences (2017-I2M-1-017, CIFMS-2021-I2M-1-001); Science and Technology Program of Nanjing, China (2019060001); Jiangsu Provincial "Double Innovation Doctors" Program (Grant No. JSSCBS20211610); Science and Technology Development Foundation of Nanjing Medical University (NMUB2020154).

Author Contributions

Supervision: Min Li; conceptualization: Meng Zhou and Yuzhen Liu; investigation: Meng Zhou, Rong Zeng, Haoxiang Xu, and Xu Chen; formal analysis: Meng Zhou, Nana Zheng, and Yiping Ge; funding acquisition: Min Li, Zhimin Duan, Yuzhen Liu, and Dongqing Li; methodology: Min Li and Tong Lin; and writing – review and editing: Meng Zhou, Rong Zeng, and Qing Chen.

Data Availability Statement

The data involved in this study are included in this article, and parts of the data are included in the supplementary information files. For further inquiries, please contact the corresponding author.

References

1 Tan JK, Bhate K. A global perspective on the epidemiology of acne. Br J Dermatol. 2015;172(Suppl 1):3–12.
2 Tilles G. Acne pathogenesis: history of concepts. Dermatology. 2014;229(1):1–46.
3 Gollnick HP. From new findings in acne pathogenesis to new approaches in treatment. J Eur Acad Dermatol Venereol. 2015;29(Suppl 5):1–7.
4 Gu H, An HJ, Gwon MG, Bae S, Leem J, Lee SJ, et al. Bee venom and its major component melittin attenuated cutibacterium acnes- and IGF-1-induced acne vulgaris via inactivation of akt/mTOR/SREBP signaling pathway. Int J Mol Sci. 2022(6):23.
5 ENCODE Project Consortium. An integrated encyclopedia of DNA elements in the human genome. Nature. 2012;489(7414):57–74.
6 Xia X, Li Z, Liu K, Wu Y, Jiang D, Lai Y. Staphylococcal LTA-induced miR-143 inhibits propionibacterium acnes-mediated inflammatory response in skin. J Invest Dermatol. 2016;136(3):621–30.

7 Zeng R, Xu H, Liu Y, Du L, Duan Z, Tong J, et al. miR-146a inhibits biofilm-derived cutibacterium acnes-induced inflammatory reactions in human keratinocytes. J Invest Dermatol. 2019;139(12):2488–96.e4.
8 Yang S, Fang F, Yu X, Yang C, Zhang X, Wang L, et al. Knockdown of H19 inhibits the pathogenesis of acne vulgaris by targeting the miR-196a/TLR2/NF-κB Axis. Inflammation. 2020;43(5):1936–47.
9 Chen LL, Yang L. Regulation of circRNA biogenesis. RNA Biol. 2015;12(4):381–8.
10 Salmena L, Poliseno L, Tay Y, Kats L, Pandolfi PP. A ceRNA hypothesis: the rosetta stone of a hidden RNA language? Cell. 2011;146(3):353–8.
11 Zheng Q, Bao C, Guo W, Li S, Chen J, Chen B, et al. Circular RNA profiling reveals an abundant circHIPK3 that regulates cell growth by sponging multiple miRNAs. Nat Commun. 2016;7:11215.
12 Piwecka M, Glažar P, Hernandez-Miranda LR, Memczak S, Wolf SA, Rybak-Wolf A, et al. Loss of a mammalian circular RNA locus causes miRNA deregulation and affects brain function. Science. 2017;357(6357):357.
13 Hao JQ. Targeting interleukin-22 in psoriasis. Inflammation. 2014;37(1):94–9.
14 Qiao M, Ding J, Yan J, Li R, Jiao J, Sun Q. Circular RNA expression profile and analysis of their potential function in psoriasis. Cell Physiol Biochem. 2018;50(1):15–27.
15 Liu X, Frost J, Bowcock A, Zhang W. Canonical and interior circular RNAs function as competing endogenous RNAs in psoriatic skin. Int J Mol Sci. 2021;22(10):5182.
16 Liang J, Wu X, Sun S, Chen P, Liang X, Wang J, et al. Circular RNA expression profile analysis of severe acne by RNA-Seq and bioinformatics. J Eur Acad Dermatol Venereol. 2018;32(11):1986–92.
17 Dong S, Wu Y, Liu Y, Weng H, Huang H. N(6) -methyladenosine steers RNA metabolism and regulation in cancer. Cancer Commun. 2021;41(7):538–59.
18 Fang Z, Mei W, Qu C, Lu J, Shang L, Cao F, et al. Role of m6A writers, erasers and readers in cancer. Exp Hematol Oncol. 2022;11(1):45.
19 Roundtree IA, Luo GZ, Zhang Z, Wang X, Zhou T, Cui Y, et al. YTHDC1 mediates nuclear export of N(6)-methyladenosine methylated mRNAs. Elife. 2017;6:e31311.
20 Kim GW, Imam H, Siddiqui A. The RNA binding proteins YTHDC1 and FMRP regulate the nuclear export of N(6)-methyladenosine-modified hepatitis B virus transcripts and affect the viral life cycle. J Virol. 2021;95(13):e0009721.
21 Chen RX, Chen X, Xia LP, Zhang JX, Pan ZZ, Ma XD, et al. N(6)-methyladenosine modification of circNSUN2 facilitates cytoplasmic export and stabilizes HMGA2 to promote colorectal liver metastasis. Nat Commun. 2019;10(1):4695.
22 Chen C, Yuan W, Zhou Q, Shao B, Guo Y, Wang W, et al. N6-methyladenosine-induced circ1662 promotes metastasis of colorectal cancer by accelerating YAP1 nuclear localization. Theranostics. 2021;11(9):4298–315.
23 Wu P, Fang X, Liu Y, Tang Y, Wang W, Li X, et al. N6-methyladenosine modification of circCUX1 confers radioresistance of hypopharyngeal squamous cell carcinoma through caspase1 pathway. Cell Death Dis. 2021;12(4):298.
24 Li M, Chen Q, Shen Y, Liu W. Candida albicans phospholipomannan triggers inflammatory responses of human keratinocytes through Toll-like receptor 2. Exp Dermatol. 2009;18(7):603–10.
25 Pillai-Kastoori L, Schutz-Geschwender AR, Harford JA. A systematic approach to quantitative Western blot analysis. Anal Biochem. 2020;593:113608.
26 Dréno B, Pécastaings S, Corvec S, Veraldi S, Khammari A, Roques C. Cutibacterium acnes (Propionibacterium acnes) and acne vulgaris: a brief look at the latest updates. J Eur Acad Dermatol Venereol. 2018;32(Suppl 2):5–14.
27 Dréno B, Dagnelie MA, Khammari A, Corvec S. The skin microbiome: a new actor in inflammatory acne. Am J Clin Dermatol. 2020;21(Suppl 1):18–24.
28 Zhong Y, Du Y, Yang X, Mo Y, Fan C, Xiong F, et al. Circular RNAs function as ceRNAs to regulate and control human cancer progression. Mol Cancer. 2018;17(1):79.
29 Zhang S, Liao K, Miao Z, Wang Q, Miao Y, Guo Z, et al. CircFOXO3 promotes glioblastoma progression by acting as a competing endogenous RNA for NFAT5. Neuro Oncol. 2019;21(10):1284–96.
30 Wu Y, Yang X, Chen Z, Tian L, Jiang G, Chen F, et al. m(6)A-induced lncRNA RP11 triggers the dissemination of colorectal cancer cells via upregulation of Zeb1. Mol Cancer. 2019;18(1):87.
31 Liu N, Dai Q, Zheng G, He C, Parisien M, Pan T. N(6)-methyladenosine-dependent RNA structural switches regulate RNA-protein interactions. Nature. 2015;518(7540):560–4.
32 Zhang L, Hou C, Chen C, Guo Y, Yuan W, Yin D, et al. The role of N(6)-methyladenosine (m(6)A) modification in the regulation of circRNAs. Mol Cancer. 2020;19(1):105.
33 Williams HC, Dellavalle RP, Garner S. Acne vulgaris. Lancet. 2012;379(9813):361–72.
34 Kircik LH. Advances in the understanding of the pathogenesis of inflammatory acne. J Drugs Dermatol. 2016;15(1 Suppl 1):s7–10.
35 Jin X, Gao J, Zheng R, Yu M, Ren Y, Yan T, et al. Antagonizing circRNA_002581-miR-122-CPEB1 axis alleviates NASH through restoring PTEN-AMPK-mTOR pathway regulated autophagy. Cell Death Dis. 2020;11(2):123.
36 Liu R, Zhang L, Zhao X, Liu J, Chang W, Zhou L, et al. circRNA: regulatory factors and potential therapeutic targets in inflammatory dermatoses. J Cell Mol Med. 2022;26(16):4389–400.
37 Cardamone G, Paraboschi EM, Rimoldi V, Duga S, Soldà G, Asselta R. The characterization of GSDMB splicing and backsplicing profiles identifies novel isoforms and a circular RNA that are dysregulated in multiple sclerosis. Int J Mol Sci. 2017;18(3):576.
38 Dong W, Bi J, Liu H, Yan D, He Q, Zhou Q, et al. Circular RNA ACVR2A suppresses bladder cancer cells proliferation and metastasis through miR-626/EYA4 axis. Mol Cancer. 2019;18(1):95.
39 Dube U, Del-Aguila JL, Li Z, Budde JP, Jiang S, Hsu S, et al. An atlas of cortical circular RNA expression in Alzheimer disease brains demonstrates clinical and pathological associations. Nat Neurosci. 2019;22(11):1903–12.
40 Shen J, Chen L, Cheng J, Jin X, Mu Y, Li Q, et al. Circular RNA sequencing reveals the molecular mechanism of the effects of acupuncture and moxibustion on endometrial receptivity in patients undergoing infertility treatment. Mol Med Rep. 2019;20(2):1959–65.
41 Li LJ, Zhu ZW, Zhao W, Tao SS, Li BZ, Xu SZ, et al. Circular RNA expression profile and potential function of hsa_circ_0045272 in systemic lupus erythematosus. Immunology. 2018;155(1):137–49.
42 O'Neill AM, Gallo RL. Host-microbiome interactions and recent progress into understanding the biology of acne vulgaris. Microbiome. 2018;6(1):177.
43 Agak GW, Mouton A, Teles RM, Weston T, Morselli M, Andrade PR, et al. Extracellular traps released by antimicrobial TH17 cells contribute to host defense. J Clin Invest. 2021;131(2):131.
44 Do TH, Ma F, Andrade PR, Teles R, de Andrade Silva BJ, Hu C, et al. TREM2 macrophages induced by human lipids drive inflammation in acne lesions. Sci Immunol. 2022;7(73):eabo2787.
45 Qu S, Yang X, Li X, Wang J, Gao Y, Shang R, et al. Circular RNA: a new star of noncoding RNAs. Cancer Lett. 2015;365(2):141–8.
46 Qiao L, Li CG, Liu D. CircRNA_0048211 protects postmenopausal osteoporosis through targeting miRNA-93-5p to regulate BMP2. Eur Rev Med Pharmacol Sci. 2020;24(7):3459–66.
47 Lv W, Tan Y, Xiong M, Zhao C, Wang Y, Wu M, et al. Analysis and validation of m6A regulatory network: a novel circBACH2/has-miR-944/HNRNPC axis in breast cancer progression. J Transl Med. 2021;19(1):527.
48 Peng F, Gong W, Li S, Yin B, Zhao C, Liu W, et al. circRNA_010383 acts as a sponge for miR-135a, and its downregulated expression contributes to renal fibrosis in diabetic nephropathy. Diabetes. 2021;70(2):603–15.
49 Chen G, Liu T, Yu B, Wang B, Peng Q. CircRNA-UBE2G1 regulates LPS-induced osteoarthritis through miR-373/HIF-1a axis. Cell Cycle. 2020;19(13):1696–705.
50 Gao L, Jin HJ, Zhang D, Lin Q. Silencing circRNA_001937 may inhibit cutaneous squamous cell carcinoma proliferation and induce apoptosis by preventing the sponging of the miRNA-597-3p/FOSL2 pathway. Int J Mol Med. 2020;46(5):1653–60.
51 Yang C, Ni B, Li C, Sun W, Wang Z, Wang H, et al. circRNA_17725 promotes macrophage polarization towards M2 by targeting FAM46C to alleviate arthritis. Mediators Inflamm. 2023;2023:6818524.